Low-temperature infrared spectroscopy of H$_2$ in crystalline C$_{60}$

S. A. FitzGerald, H. O. H. Churchill, P. M. Korngut, C. B. Simmons, and Y. E. Strangas

Department of Physics and Astronomy, Oberlin College, Oberlin, Ohio, 44074, USA

(Received 6 February 2006; published 7 April 2006)

Diffuse reflectance infrared spectroscopy is used to measure the quantum dynamics of molecular hydrogen trapped within a C$_{60}$ lattice at temperatures as low as 10 K. Crystal field effects in conjunction with rotational translational coupling lead to a rich spectrum with multiply split peaks that are more than an order of magnitude sharper than at room temperature. The induced redshifts in the vibrational-rotational mode frequencies are explained using a simple model in which the state dependence of the H$_2$ polarizability leads to changes in the C$_{60}$-H$_2$ interaction potential.

I. INTRODUCTION

There is presently much interest in hydrogen storage for fuel cell applications.[1–3] The ultimate goal of this research is to obtain a light-weight matrix that can hold significant quantities of molecular hydrogen at room temperature. In trying to develop these materials it is necessary to do more than simply measure the quantity of hydrogen a material will hold. It is essential that we understand the details of the intermolecular interactions that bind molecular hydrogen to a host.

One such host that has attracted much recent attention is the C$_{60}$ fullerene lattice.[4–13] Although the low hydrogen uptake of C$_{60}$ relative to its large mass makes it an unlikely material for practical hydrogen storage, it is an ideal system to study the carbon hydrogen intermolecular interaction and its effect on the quantum dynamics of confined H$_2$. It is now well established that H$_2$ binds solely at the fullerene interstitial lattice site with octahedral symmetry.[6] The site appears to be just large enough to hold a single H$_2$ molecule with a negligible amount of multiple occupancy.[10] Because neighboring octahedral sites are well separated (10 Å) there is almost no H$_2$-H$_2$ interaction, and the system can be treated as an ideal case of an isolated molecule within a cavity. The low mass of the H$_2$ molecule combined with the highly isotropic confining potential means that quantum effects dominate for both the center of mass motion and the nearly free molecular rotations that occur even at the lowest of temperatures.

To date inelastic neutron scattering,[4,6,14] nuclear magnetic resonance (NMR) spectroscopy,[7] Raman scattering,[9] and infrared (IR) spectroscopy[8] have all been used to investigate the quantum dynamics of the trapped H$_2$. In addition there have been comprehensive theoretical studies of the C$_{60}$-H$_2$ interaction potential.[10,13–15] Despite these efforts our understanding of the system is still somewhat limited. Neither NMR nor Raman scattering experiments were able to directly probe the center of mass motion of the trapped H$_2$. The neutron scattering results were limited by overlapping peaks and an insufficient instrument resolution. Our original infrared work was able to observe a series of vibrational, rotational, and center of mass translational bands arising from the trapped H$_2$. However, because the spectra could only be obtained at room temperature the peaks were quite broad and

overlapping. This limited the degree to which the data could be used to put constraints on the proposed theoretical models.

As a homonuclear diatomic molecule H$_2$ has no dipole moment and is IR inactive. Any IR activity arises from the presence of induced dipole moments formed by the interactions between hydrogen and the host.[16] As such the IR spectrum is extremely sensitive to the details of the host adsorbate intermolecular potential. The drawback that the induced dipole moment is quite small and thus the spectrum quite weak can be overcome by the use of diffuse reflectivity.[8] The diffuse reflectance infrared Fourier transform spectroscopy (DRIFTS) technique achieves a very long optical path length within a highly scattering but transparent host material such as C$_{60}$. This dramatically increases the observed signal over that obtained using traditional transmission measurements.

Our initial room temperature spectra exhibited a series of broad absorbance peaks in the frequency region of the rotational-vibrational spectrum of pure gas phase H$_2$.[8] The spectrum showed a pattern of two strong sidebands placed symmetrically in frequency about a much weaker central peak. We tentatively assigned the sidebands to transitions in which the H$_2$ either gained or lost one unit of quantized translational energy due to the center of mass motion of the H$_2$ within the octahedral void. However, due to the overlapping nature of the peaks it was impossible to perform an unambiguous mode assignment. In this paper we show how these problems are overcome by obtaining spectra at liquid helium temperature.

In the next section we present a theoretical basis for the interaction-induced frequency shifts and IR selection rules governing the H$_2$ in C$_{60}$ vibrational-rotational-translational spectrum. Section III contains an outline of our procedure using a custom designed cryostat to obtain DRIFT spectra at liquid helium temperature. The resulting spectra which are dramatically sharper than those at room temperature are presented in the results section. Finally the data are analyzed with respect to the model predictions of Yildirim and Brooks[14] and Herman and Lewis.[15]

II. THEORY

A free H$_2$ molecule has a fundamental vibrational frequency for the $\nu=0$ to $\nu=1$ transition of 4161 cm^{-1} and in

addition acts as a near perfect quantum rotor with rotational energy levels

$$E(J) = B_\nu J(J+1), \qquad (1)$$

where J is the rotational quantum number and B_ν, the rotational constant, is 59 cm^{-1} for hydrogen in its ground vibrational state.[17] Quantum statistics constrain the total nuclear wave function to be odd under nuclear exchange. As such those molecules with total nuclear spin $I=1$ must have an even J quantum number. This is referred to as orthohydrogen. Similarly parahydrogen with nuclear spin $I=0$ is constrained to have an odd J.

The effect of the C_{60} confining potential modifies both the vibrational and rotational constants and in addition lifts the degeneracy of the rotational levels.[14] However, the orthopara antisymmetry constraint is still maintained which fundamentally limits all photon induced transitions to those with $\Delta J =0$ (Q transitions) and $\Delta J = \pm 2$ (S and O transitions).[18]

The center of mass motion of a hydrogen molecule confined to a C_{60} octahedral site has been modeled as that of a perturbed isotropic harmonic oscillator. Yildirim and Harris[14] describe the system with spherical coordinates while Herman and Lewis[15] use Cartesian. The starting point for both models is entirely equivalent, but they diverge once the perturbing terms are added. In the case of Yildirim and Harris,[14] the quantum numbers are the principal quantum number N with rotational quantum numbers L and m_L. For Herman and Lewis[15] the three quantum numbers are n_x, n_y, and n_z.

The C_{60}-H_2 interaction potential gives rise to a frequency shift, $\Delta\nu$, relative to free H_2. For a transition between energy states E_i and E_f, the shift is

$$\Delta\nu = \nu_H - \nu_G$$

$$= \frac{1}{h}[(E_f - E_i)_H - (E_f - E_i)_G]$$

$$= \frac{1}{h}[(E_H - E_G)_f - (E_H - E_G)_i], \qquad (2)$$

where the subscripts H and G refer to H_2 in the C_{60} host and in the gas phase, respectively. The energy differences in (2) may be treated using first order perturbation theory. Ignoring rotational-translational coupling, we have

$$(E_H - E_G)_f = \langle \nu=1, J_f, n | V | \nu=1, J_f, n \rangle,$$

$$(E_H - E_G)_i = \langle \nu=0, J_i, n | V | \nu=0, J_i, n \rangle \qquad (3)$$

for zero-phonon transitions in which $n_i = n_f = n$, where V is the C_{60}-H_2 interaction potential. Writing (3) more compactly and substituting into (2), the frequency shift is

$$\Delta\nu = \frac{1}{h}(\langle V \rangle_f - \langle V \rangle_i). \qquad (4)$$

The observed frequency shift is a tradeoff between the redshift of the attractive part of the potential and the blueshift of the repulsive part[19] so that (4) may be separated as

$$\Delta\nu = \Delta\nu_a + \Delta\nu_r, \qquad (5)$$

where[20]

$$\Delta\nu_a = \frac{\alpha_{1,J_f} - \alpha_{0,J_i}}{\alpha_{0,J_i}} \langle V_a \rangle_i, \qquad (6a)$$

$$\Delta\nu_r = \frac{\alpha_{1,J_f} - \alpha_{0,J_i}}{\alpha_{0,J_i}} \left(\frac{2+y}{1+y} \right) \langle V_r \rangle_i. \qquad (6b)$$

Here $\langle V_a \rangle_i$ and $\langle V_r \rangle_i$ are the expected values of the attractive and repulsive parts of the interaction potential in the initial state, and α_{0,J_i} and α_{1,J_f} are the polarizabilities of the H_2 molecule in the initial and final states. The empirical parameter y has a value of about 10 for C_{60}-H_2[20,21] so if V were dominated by the repulsive part, the term in parentheses in (6b) would represent a 10% contribution to $\Delta\nu$. However, using previous models for the C_{60}-H_2 interaction potential,[6,15] we find that $\langle V \rangle$ is dominated by the attractive part for all thermally populated translational states at room temperature and below. Thus to within 1–2%, the term in parentheses in (6b) may be ignored, and combining the two contributions to the frequency shift gives us

$$\Delta\nu \approx \frac{\alpha_{1,J_f} - \alpha_{0,J_i}}{\alpha_{0,J_i}} \langle V \rangle_i. \qquad (7)$$

Modeling the translational motion of H_2 in C_{60} as an isotropic three-dimensional harmonic oscillator, the frequency shift for transitions originating in translational state n is

$$\Delta\nu = \frac{\alpha_{1,J_f} - \alpha_{0,J_i}}{\alpha_{0,J_i}} \left[E_0 + \frac{1}{2}\left(n + \frac{3}{2}\right)\hbar\omega \right], \qquad (8)$$

where E_0 is the C_{60}-H_2 potential minimum and $\hbar\omega$ is the spacing between translational levels.[19]

Because H_2 has no intrinsic IR activity any observed absorption spectrum arises solely through dipole moments induced by interactions with the host material. These can arise from van der Waals interactions in which the host field induces a dipole moment on the H_2, or from the H_2 quadrupole moment inducing a dipole moment on the host atoms.[22] In either case the total induced dipole moment is zero if the H_2 sits at a point of inversion symmetry such as the center of the C_{60} octahedral site.[22] In a classical picture, inversion symmetry is destroyed by the center of mass motion of the H_2 off center. Quantum mechanically this results in predictions that the IR spectrum of H_2 in C_{60} will be dominated by modes in which the H_2 undergoes a change in its translational quantum numbers.[23] Herman and Lewis[15] state selection rules of $\Delta n_z = \pm 1$ with $\Delta n_x = \Delta n_y = 0$. Similarly, either n_x or n_y could change, but transitions in which two or more of the quantum numbers change are discounted. For the spherical coordinate notation of Yildirim and Brooks[14] the equivalent selection rules are $\Delta N = \pm 1$ with $\Delta L = \pm 1$ to maintain parity.

Figure 1 illustrates the allowed transitions for a temperature in which only the ground and first translational excited states are populated. In the absence of ortho to para conversion 3/4 of the molecules are trapped in the rotational excited $J=1$ state. Transitions in which the translational quantum number increases by 1 are called R transitions and those in which it decreases by 1, P transitions. At liquid helium
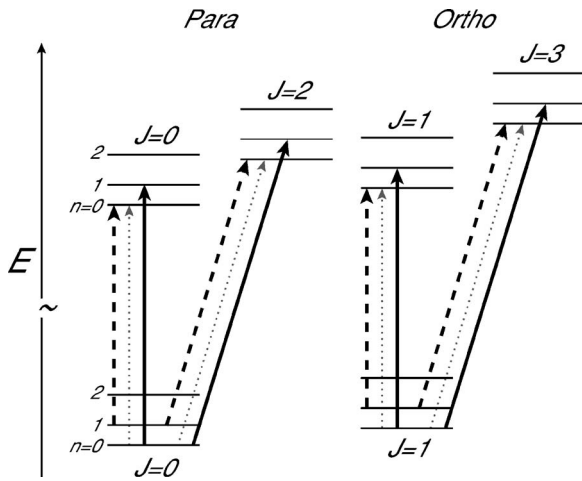
FIG. 1. Energy level scheme for the fundamental vibrational transition of H$_2$ in C$_{60}$. The rotational selection rules are $\Delta J = 0$ (Q transitions) and $\Delta J = +2$ (S transitions). The dominant features of our spectra are translational sidebands with $\Delta n = +1$ (R branch, solid lines) and $\Delta n = -1$ (P branch, dashed lines). Weak transitions are also observed with $\Delta n = 0$ (Q branch, dotted lines). The anharmonicity of the translational levels has been exaggerated for illustration.

temperature only the translational ground state is populated, and we would expect to observe only four transitions labeled as $Q_R(0)$, $Q_R(1)$, $S_R(0)$, and $S_R(1)$, where the number in parentheses refers to the initial rotational quantum number J.

III. EXPERIMENTAL PROCEDURE

The custom built cryostat used in this work is the subject of another paper, and we present only a brief summary of its design below. A commercially obtained DRIFTS accessory consisting of a series of collecting optics was bolted inside a large optical access vacuum chamber ($12 \times 20 \times 15$ cm). A cold finger cryostat (modified Janis ST-300T) was inserted into the chamber via a 3.8 cm compression seal. A 6 mm thick copper slab was mounted at the base of the cold finger. The slab was 9 cm in length and contained a soldered sample cup at the far end from the cold finger. A high-pressure capillary line was also attached to the copper slab and entered the vacuum chamber via a second compression fitting. The sample cup was surrounded by a high-pressure ZnSe dome that allowed transmission in the mid-IR. Silicon diode thermometers were mounted at the base of the cold finger and by the sample at the far end of the copper slab.

All spectra were obtained using a Bomem DA3 Michelson interferometer with globar source and a KBr beam splitter. We used a liquid nitrogen cooled mercury cadmium telluride detector. The spectrometer has a maximum resolution of 0.04 cm^{-1}, but the highest resolution used for this work was 0.2 cm^{-1}.

Loading of hydrogen within a C$_{60}$ powder is complicated by the fact that the kinetics for hydrogen diffusion within the C$_{60}$ lattice are extremely slow even at room temperature.[24] Loading at temperatures significantly below ambient is practically infeasible due to the excessive time scale. In our case we used C$_{60}$ crystallites obtained commercially from MER Corporation consisting of highly twinned particles with dimensions on the order of a few millimeters.

The sample was initially subject to a loading pressure of 100 atm at room temperature. This pressure was maintained for three days while spectra were taken to monitor the adsorption of H$_2$ within the sample. The results were quite similar to those published previously[8] except that the time scale for H$_2$ diffusion was much longer due to the increased size of the C$_{60}$ crystallites. After three days the high-pressure dome was removed, the vacuum chamber evacuated, and the sample cooled to 10 K. This entire procedure took less than 15 min during which time it was assumed that only a small fraction of the trapped H$_2$ escaped from the sample.

IV. RESULTS

Figure 2 shows the low temperature absorption spectra arising from H$_2$ trapped within the C$_{60}$ lattice. The spectra are referenced to that of the pure C$_{60}$ sample at the same
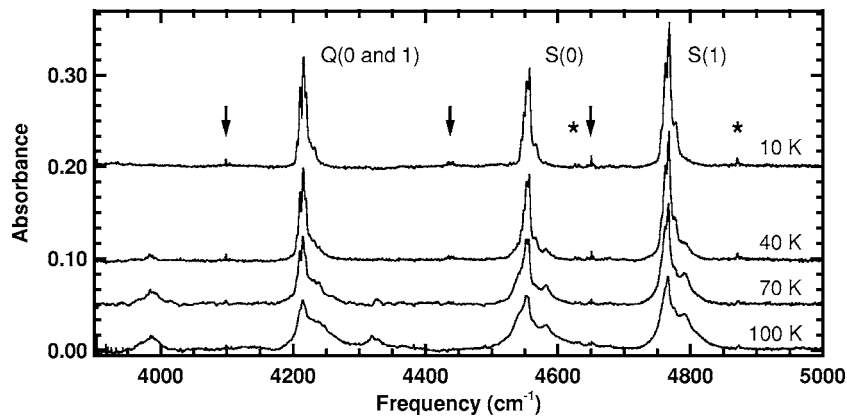

FIG. 2. Temperature dependence of DRIFT spectra of the fundamental vibrational transition of H$_2$ in C$_{60}$. The most prominent features of the spectra are translational-rotational sidebands with $\Delta n = +1$ and $\Delta J = 0$, $+2$. The arrows mark the positions of the weak zero-phonon modes that lie midway between the P and R translational sidebands. The asterisks mark features that we are confident arise from trapped H$_2$ excitations but were not able to assign.

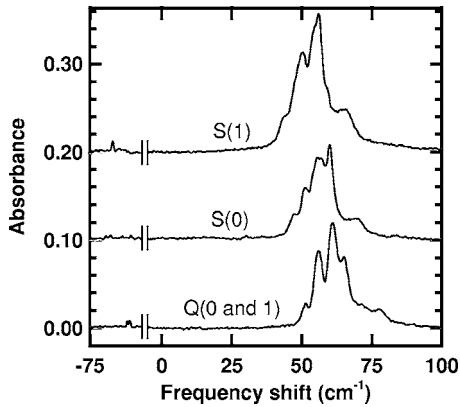FIG. 3. Zero-phonon and *R*-branch ($\Delta n = +1$) for $Q(0$ and $1)$, $S(0)$, and $S(1)$ obtained at 10 K. The frequencies have been shifted by the corresponding values for gas phase H_2: $Q(0$ and $1)$ by 4155.3 cm^{-1}, $S(0)$ by 4497.8 cm^{-1}, and $S(1)$ by 4712.9 cm^{-1}.

temperature. At the lowest temperature of 10 K the spectrum contains three main features, each with a significant fine structure. In all cases the observed peaks arise from the H_2 fundamental vibrational mode, with additional changes in rotational and/or translational quantum states of the trapped H_2. As stated in the theory section, at 10 K only the translational ground state, $n=0$, is thermally populated. Due to the lack of ortho to para conversion both the $J=0$ and $J=1$ rotational levels are populated even at the lowest temperature and we expect to observe sets of peaks corresponding to $Q_R(0)$, $Q_R(1)$, $S_R(0)$, and $S_R(1)$ transitions. The $Q(0)$ and $Q(1)$ transitions are only separated by 6 cm^{-1} in free H_2 (Ref. 17) which is significantly less than the splitting caused by the C_{60} interactions. Hence it is not surprising that they appear as a single feature in our overview spectrum. In the future we will refer to this feature simply as the Q band.

On warming the excited state translational levels become thermally populated, and we observe a progressive broadening in the main features with a definite asymmetry toward the higher frequency side. This is consistent with the predictions of Yildirim and Harris[14] and Herman and Lewis[15] that the translational levels possess a large anharmonicity with an increasing level spacing.

Populating the translational excited states also leads to the presence of P transitions with $\Delta n = -1$. These are most obvious for the Q_P transition centered at 3985 cm^{-1} and the $S_P(0)$ at 4325 cm^{-1}. The expected $S_P(1)$ transition is obscured by the main $S_R(0)$ feature at 4550 cm^{-1}.

The midpoint frequency of the R and P transitions should correspond to the frequency of the so called zero-phonon or pure rotational-vibrational modes in which there is no translational transition and $\Delta n = 0$. The arrows in Fig. 2 indicate the midpoint frequencies based on the center of area of the P and R bands, and in each case we observe a weak but quite sharp set of bands at these frequencies.

As shown in Fig. 3 these pure rotational-vibrational transitions are redshifted relative to their gas phase values. For the Q band we used the $Q(1)$ gas phase value as our reference frequency since it is expected to dominate over the $Q(0)$ in the absence of ortho to para conversion.[25] We ob-

serve a doublet peak at -57 cm^{-1} that we attribute to $Q(1)$ with a much weaker peak 6 cm^{-1} higher in frequency which would be consistent with a $Q(0)$ transition. The $S(0)$ features are all quite weak and in some cases it appears that the peaks arose from imperfect cancellation with the C_{60} reference spectrum. However, we are confident that there are at least four H_2 peaks centered at -60 cm^{-1}. For the $S(1)$ transition there is a prominent peak at -63 cm^{-1} with additional absorption on either side of the peak. In general the peaks have full width at half maximum (FWHMs) on the order of 0.5–1 cm^{-1} which are considerably sharper than those associated with the translational R peaks appearing on the right-hand side of the graph.

The R-branch locations can be crudely understood in terms of the pure vibrational-rotational redshift plus the center of mass translational frequency. Using the center of area to define a single frequency we see a systematic increase in the frequency shift on going from Q to $S(0)$ to $S(1)$ that is virtually identical to that of the zero-phonon modes on the left-hand side of the graph. From this we conclude that the trend arises from a systematic change in the rotational energy rather than a rotational-translational coupling.

V. ANALYSIS AND DISCUSSION

A. Frequency redshift

The vibrational and rotational state dependence of the redshifts can be understood using the model presented in Sec. II. The redshifts arise from differences in the polarizability of H_2 in its initial and final rotational-vibrational states. Because the polarizability of H_2 is greater in excited states[26] and because the binding energy defined in Eq. (8) is negative for all thermally populated translational levels at room temperature and below, the model predicts highly redshifted spectra for all observed transitions. Using the previously measured room temperature value of E_0 for H_2 in C_{60}[8] in conjunction with the polarizability values derived by Kolos *et al.*,[26] we estimate the room temperature redshifts to be -50, -53, and -55 cm^{-1} for the Q, $S(0)$, and $S(1)$ transitions, respectively. These agree quite well with the measured values of -49, -52, and -55 cm^{-1}.

Experimentally we see an increase in the magnitude of the redshift on cooling to 10 K, with the values now being -57, -60, and -63 cm^{-1} for Q, $S(0)$, and $S(1)$, respectively. The redshift depends on temperature not only because of changing occupancy of translational states but also because E_0 is affected by lattice contraction. The C_{60} lattice contracts by 1% upon cooling from room temperature to 10 K.[27] Assuming a 12-6 or exp-6 model for the interaction potential, this contraction results in a 5% increase in the magnitude of E_0 from which we estimate redshifts at 10 K of -60, -64, and -66 cm^{-1}. These are all consistently larger than the observed values. Given the crudeness of our estimate for E_0 at 10 K it is not surprising that there is a slight discrepancy with the model predictions.

An alternate description of the redshift process is that interactions with the C_{60} lattice stretches the H_2 bond length leading to the decreased vibrational frequency.[28] The in-
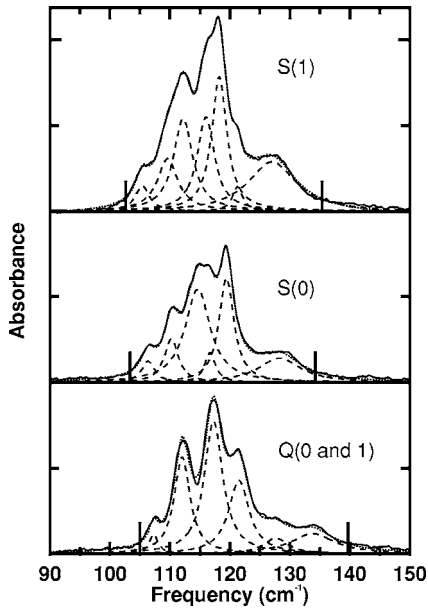
FIG. 4. R-branch fine structure of the $Q(0$ and $1)$, $S(0)$, and $S(1)$ transitions (solid lines) at 10 K fit to sum (dotted lines) of Lorentzian line shapes (dashed lines). The spectra have been shifted by the center frequency of the corresponding zero-phonon modes, $Q(0$ and $1)$ by 4098.5 cm^{-1}, $S(0)$ by 4438 cm^{-1}, and $S(1)$ by 4650.4 cm^{-1}, to show the frequency of the translational transition. The R-branches of $Q(0$ and $1)$ and $S(0)$ were fit to a sum of six Lorentzians. $S(1)$ required a sum of seven Lorentzians to achieve a satisfactory fit. The fit parameters are listed in Table I. The vertical bars illustrate the effective width of the bands.

TABLE I. Frequencies, FWHMs, and relative intensities of the Q_R, $S_R(0)$, and $S_R(1)$ transitions of H₂ in C₆₀ at 10 K fit to Lorentzian line shapes. Frequencies have been shifted by the zero-phonon values of 4098.5, 4438, and 4650.4 cm^{-1}, respectively.

	Frequency (cm^{-1})	FWHM (cm^{-1})	Rel. Intensity
	107	1.8	0.07
	112	3.2	0.63
Q	117	3.7	1.00
	122	4.1	0.62
	128	5.0	0.16
	134	8.9	0.37
	106	2.7	0.12
	110	2.9	0.26
$S(0)$	115	5.1	1.00
	117	2.2	0.14
	119	3.0	0.67
	128	8.7	0.44
	105	2.7	0.14
	110	4.1	0.44
	112	3.9	0.72
$S(1)$	116	3.5	0.66
	118	3.1	0.84
	121	2.0	0.10
	127	9.9	1.00

creased bond length also reduces the rotational constants by an estimated 1.2% corresponding to 0.7 cm^{-1} for B_0. This leads to the observed increase in redshift on moving from Q to $S(0)$ to $S(1)$.

B. Translational sidebands

To explore the translational modes in more detail we subtracted off the zero-phonon center of area frequency for the Q, $S(0)$, and $S(1)$ transitions, respectively. The spectra as shown in Fig. 4 thus represent the translational mode contribution to the transition energy. Plotted in this way the three sets of bands are quite similar. Each is split into at least six peaks, with the center of area lying at 118 cm^{-1} in all cases. The effective spread in frequency of the three bands (as indicated by the vertical lines in the figure) range from 35 cm^{-1} for Q_R to 31 and 32 cm^{-1} for $S_R(0)$ and $S_R(1)$, respectively. The slightly greater width for Q_R may be due to the presence of a small amount of $Q_R(0)$ which should occur 6 cm^{-1} higher in frequency than the dominant $Q_R(1)$.

There have been several attempts to determine the fundamental translational energy of H₂ trapped in C₆₀. Tomaselli and Meier[7] used NMR measurements to estimate a value of 105 cm^{-1}, while neutron scattering showed peaks centered around 113 cm^{-1} (Ref. 6). Theoretically Yildirim and Harris[14] predicted a value of 113 cm^{-1}, while Herman and Lewis[15] derived a room temperature value of 96 cm^{-1} that we believe corresponds to a frequency of 110 cm^{-1} at 10 K.

In each case our frequency values are somewhat higher than these, being centered at 118 cm^{-1}. We believe this reflects a real difference based on the fact that the R transitions probe the translational energy in the H₂ vibrational excited state where the increased polarizability leads to a slight increase in the translational energy. This explanation is supported by an examination of the P transitions, where the frequency difference with the zero-phonon modes represents the translational energy in the H₂ vibrational ground state. In this case we do obtain an average frequency of 113 cm^{-1}, consistent with previous results.

A detailed theoretical explanation of the fine structure present in the translational modes is beyond the scope of this paper. Our aim is to present the results of a simple deconvolution of the spectra which can be used by others to significantly improve the existing models of the H₂-C₆₀ system. Our findings are summarized in Table I and Fig. 4.

In agreement with the predictions of Herman and Lewis[15] we find that Lorentzian line profiles produce a substantially better fit to the data than Gaussian. From this we conclude that the widths are the result of lifetime broadening or dephasing effects rather than site inhomogeneity. The FWHMs are typically on the order of 3–4 cm^{-1} with in each case a much broader shoulder on the high frequency side. These widths are significantly higher than those observed for the zero-phonon modes, 0.5 to 1 cm^{-1}, and presumably reflect the fact that the individual bands are composed of multiple modes and that the relaxation process is enhanced for

translationally excited states. Most likely this occurs through relaxation within the given multiplet levels via coupling to C_{60} lattice phonons.

The widths obtained for the zero-phonon modes of H_2 trapped in rare gas matrices are comparable being on the order of 0.5 to 1 cm^{-1} (Ref. 29). However, the translational sidebands are approximately a factor of two wider than those of H_2 in C_{60}.

The translational mode splittings are predicted to arise from a combination of crystal field effects and rotational-translational coupling.[14] Crystal field effects lift the degeneracy of the pure rotational J levels such that at low temperature $J=1$ is split into two, $J=2$ split into three, and $J=3$ split into four distinct energy states. Similarly, the $n=1$ translational state is split into two levels. Once rotational-translational coupling is taken into account the picture becomes more complex. For example the $J=1$, $n=1$ state is predicted to have six separate energy levels.[14] From this perspective it is not surprising that the spectra contain a rich fine structure.

The fact that the three modes shown in Fig. 4 have similar widths can be attributed to the fact that although the number of sublevels increases with increasing J, the magnitude of the splitting is quite similar. For example $J=1$ is known to be split into two levels separated by 6 cm^{-1} while $J=3$ is split into four sublevels with a predicted energy difference from lowest to highest of just 7 cm^{-1}.

C. Zero-phonon band

Finally, we consider the origin of the weak zero-phonon modes. In principle these $\Delta n=0$ transitions should not be observed since the center of the octahedral site is a point of inversion symmetry. For H_2 in argon a localized crystal transformation from fcc to hcp was evoked to explain the

origin of similarly weak zero-phonon bands.[23] This appears unlikely in the case of C_{60} although a localized lattice deformation cannot be ruled out. The known persistence of a low temperature merohedral disorder in C_{60} would destroy perfect inversion symmetry although the reduction in symmetry would be very minor and has generally been ignored in theoretical models.[14,15] It is also possible that the modes arise from the presence of impurities or defects such as C_{60} vacancies. However, it should be noted that the zero-phonon modes occur at the midpoint of the P and R ($\Delta n=\pm 1$) branches, indicating that the H_2 is sitting at a similar site to that of the main features.

VI. CONCLUSION

In conclusion we have demonstrated the advantage of using the DRIFTS technique to obtain weak IR impurity spectra at temperatures as low as 10 K. For H_2 in C_{60} the frequency shifts of the pure vibrational-rotational modes are explained by a simple model based on changes in H_2 polarizability. The translational sidebands contain a rich substructure which we hope will be used by theorists to further reduce the uncertainties in the C-H interaction potential. Finally, we note that this application of DRIFTS seems quite feasible with H_2 in other host systems such as MOF-5 and we expect that it will be used for many such studies.

[1] L. Schlapbach and A. Züttel, Nature (London) **414**, 353 (2001).

[2] M. S. Dresselhaus, G. W. Crabtree, and M. V. Buchanan, MRS Bull. **30**, 518 (2005).

[3] M. Fichtner, Adv. Eng. Mater. **7**, 443 (2005).

[4] A. I. Kolesnikov, V. E. Antonov, I. O. Bashkin, G. Grosse, A. P. Moravsky, A. Y. Muzychka, E. G. Ponyatovsky, and F. E. Wagner, J. Phys.: Condens. Matter **9**, 2831 (1997).

[5] I. Holleman, G. von Helden, A. van der Avoird, and G. Meijer, Phys. Rev. Lett. **80**, 4899 (1998).

[6] S. A. FitzGerald, T. Yildirim, L. J. Santodonato, D. A. Neumann, J. R. D. Copley, J. J. Rush, and F. Trouw, Phys. Rev. B **60**, 6439 (1999).

[7] M. Tomaselli and B. H. Meier, J. Chem. Phys. **115**, 11017 (2001).

[8] S. A. FitzGerald, S. Forth, and M. Rinkoski, Phys. Rev. B **65**, 140302(R) (2002).

[9] K. A. Williams, B. K. Pradhan, P. C. Eklund, M. K. Kostov, and M. W. Cole, Phys. Rev. Lett. **88**, 165502 (2002).

[10] B. P. Uberuaga, A. F. Voter, K. K. Sieber, and D. S. Sholl, Phys. Rev. Lett. **91**, 105901 (2003).

[11] B. Sundqvist, Low Temp. Phys. **29**, 440 (2003).

[12] A. V. Talyzin and S. Klyamkin, Chem. Phys. Lett. **397**, 77 (2004).

[13] J. D. Turnbull and M. Boninsegni, Phys. Rev. B **71**, 205421 (2005).

[14] T. Yildirim and A. B. Harris, Phys. Rev. B **66**, 214301 (2002).

[15] R. M. Herman and J. C. Lewis, Phys. Rev. B **73**, 155408 (2006).

[16] J. Vitko and C. F. Coll, J. Chem. Phys. **69**, 2590 (1978).

[17] S. L. Bragg, J. W. Brault, and W. H. Smith, Astrophys. J. **263**, 999 (1982).

[18] G. Herzberg, *Molecular Spectra and Molecular Structure*, Spectra of Diatomic Molecules (Kriegler Publishing Company, Florida, 1989), Vol. I, reprint ed.

[19] C. M. Hartwig and J. Vitko, Jr., Phys. Rev. B **18**, 3006 (1978).

[20] *Vibrational Spectroscopy of Trapped Species*, edited by H. E. Hallam (Wiley, New York, 1973).

[21] A. Cheng, M. L. Klein, and C. Caccamo, Phys. Rev. Lett. **71**, 1200 (1993).

[22] J. V. Kranendonk, *Solid Hydrogen* (Plenum Press, New York 1983).

[23] R. J. Kriegler and H. L. Welsh, Can. J. Phys. **46**, 1181 (1968).

[24] S. A. FitzGerald, R. Hannachi, D. Sethna, M. Rinkoski, K. K. Sieber, and D. S. Sholl, Phys. Rev. B **71**, 045415 (2005).

[25] V. F. Sears and J. V. Kranendonk, Can. J. Phys. **42**, 980 (1964).

[26] W. Kolos and L. Wolniewicz, J. Chem. Phys. **46**, 1426 (1967).

[27] W. I. F. David, R. M. Ibberson, T. J. S. Dennis, J. P. Hare, and K.

Prassides, Europhys. Lett. **3**, 219 (1992).

[28] R. J. L. Roy and J. V. Kranendonk, J. Chem. Phys. **61**, 4750 (1974).

[29] M. E. Alikhani, B. Silvi, J. P. Perchard, and V. Chandrasekharan, J. Chem. Phys. **90**, 5221 (1989).